Arsenic-Induced Enhancement of Ultraviolet Radiation Carcinogenesis in Mouse Skin: A Dose–Response Study

Fredric J. Burns, Ahmed N. Uddin, Feng Wu, Arthur Nádas, and Toby G. Rossman

Department of Environmental Medicine, School of Medicine, New York University, Tuxedo, New York, USA

The present study was designed to establish the form of the dose–response relationship for dietary sodium arsenite as a co-carcinogen with ultraviolet radiation (UVR) in a mouse skin model. Hairless mice (strain Skh1) were fed sodium arsenite continuously in drinking water starting at 21 days of age at concentrations of 0.0, 1.25, 2.5, 5.0, and 10 mg/L. At 42 days of age, solar spectrum UVR exposures were applied three times weekly to the dorsal skin at 1.0 kJ/m^2 per exposure until the experiment ended at 182 days. Untreated mice and mice fed only arsenite developed no tumors. In the remaining groups a total of 322 locally invasive squamous carcinomas occurred. The carcinoma yield in mice exposed only to UVR was 2.4 ± 0.5 cancers/mouse at 182 days. Dietary arsenite markedly enhanced the UVR-induced cancer yield in a pattern consistent with linearity up to a peak of 11.1 ± 1.0 cancers/mouse at 5.0 mg/L arsenite, representing a peak enhancement ratio of 4.63 ± 1.05. A decline occurred to 6.8 ± 0.8 cancers/mouse at 10.0 mg/L arsenite. New cancer rates exhibited a consistent-with-linear dependence on time beginning after initial cancer-free intervals ranging between 88 and 95 days. Epidermal hyperplasia was elevated by arsenite alone and UVR alone and was greater than additive for the combined exposures as were growth rates of the cancers. These results demonstrate the usefulness of a new animal model for studying the carcinogenic action of dietary arsenite on skin exposed to UVR and should contribute to understanding how to make use of animal data for assessment of human cancer risks in tissues exposed to mixtures of carcinogens and cancer-enhancing agents. *Key words:* **arsenic, arsenite, cancer, hairless, mouse, radiation, skin, ultraviolet, UV.** *Environ Health Perspect* **112:599–603 (2004). doi:10.1289/ehp.6655 available via *http://dx.doi.org/* [Online 6 January 2004]**

Although elevated cancer risk has been demonstrated in people exposed to arsenic in drinking water, the data generally cannot distinguish between various possible dose–response relationships, such as linear, quadratic, or hockey stick (Buchet and Lison 2000). However, studies of skin or bladder cancer among persons consuming arsenic-contaminated drinking water in Taiwan were consistent with linearity, although other forms could not be ruled out (Brown et al. 1989, 1997; Chiou et al. 2001). Lung cancer in smelter workers was consistent with linear when analyzed according to the excess mortality approach but not when analyzed according to the standard mortality approach (Viren and Silvers 1999).

In other studies, dose–response tended to be hockey stick shaped at low levels of arsenic (~ < 100 ppb) in drinking water for skin cancer and for non-neoplastic end points, such as hyperpigmentation and keratosis (Tucker et al. 2001). Males were considerably more susceptible than females, and low body weight, presumably a result of poor nutrition, was predisposing (Guha Mazumder et al. 1998). Although solar keratosis is a benign neoplastic condition thought by some to be a precursor of squamous cell carcinomas, no direct linkage was apparent in these studies. Overall, the human data are not yet sufficient to contest the low-dose linearity default form of the dose–response relationship for cancer induction by arsenite (Huff et al. 1998).

Numerous ideas have been put forward to explain arsenic's carcinogenic activity (Abernathy et al. 1999; Corsini et al. 1999; Germolec et al. 1997; Rossman 2003; Rossman et al. 2002; Simeonova and Luster 2000; Yager and Wiencke 1993, 1997). Possible mechanisms include reduced DNA repair, altered DNA methylation, increased growth factors, enhanced cell proliferation, induction of gene amplification (an indication of genomic instability), and suppressed p53 expression leading to faulty DNA damage signaling (which also affects repair). In support of the latter, it was recently found that arsenite prevented S-phase arrest in human lung tumor cells irradiated with ultraviolet C radiation (UV-C; Hartwig et al. 2002). Although proliferation is a requisite of skin tumor promotion (Schlatterer et al. 2000), work with transgenic mice indicates that arsenic has little or no tumor-promoting activity (Germolec et al. 1998).

Arsenic is carcinogenic without binding to DNA, although at higher doses deletion mutations, typically associated with oxidative DNA damage, occur (Bau et al. 2002; Hei et al. 1998). One of the most puzzling aspects of arsenic carcinogenesis has been the high susceptibility of humans and the seeming refractoriness of laboratory animals to arsenic in drinking water (National Research Council 1999). A clue to the mechanism of arsenite's carcinogenic action was derived from *in vitro* mutagenesis studies with Chinese hamster fibroblasts (V-79 cells). Arsenite, not mutagenic by itself, enhanced the mutagenicity of carcinogens, such as ultraviolet radiation (UVR) and methylnitrosourea (Li and Rossman 1989b; Rossman 1989). This so-called co-mutagenic effect of arsenite was based on an inhibition of the ligation step in base excision repair (Li and Rossman 1989a, 1991), although direct inactivation of the ligase itself was ruled out (Rossman 1981; Hu et al. 1998).

Human osteogenic sarcoma cells exhibited delayed mutagenesis after many generations of exposure to extremely low concentrations (< 0.1 μM) of arsenite (Mure et al. 2003). Studies with normal human fibroblasts *in vitro* have shown that arsenite at low concentrations (0.1 μM) interferes with p53 signaling and causes up-regulation of cyclin D1 (Vogt and Rossman 2001). The latter finding raises the possibility that arsenite may reverse the p53-dependent proliferation blockage typically associated with DNA-damaging agents.

Other possible mechanisms exist. For example, mouse Hepa-1 cells exposed to benzo[*a*]pyrene *in vitro* exhibited an 18-fold increase of DNA adducts in the presence of arsenite compared with no arsenite. The rate of adduct removal was not affected, implying that arsenite acted before adduct removal in this system (Maier et al. 2002).

The present study was designed to establish the shape of the dose–response relationship for cancer enhancement in a new mouse skin model using arsenite in drinking water in combination with chronic topical UVR exposures (Rossman et al. 2001).

Address correspondence to F.J. Burns, New York University, School of Medicine, Department of Environmental Medicine, 57 Old Forge Rd., Tuxedo, NY 10987 USA. Telephone: (845) 731-3551. Fax: (845) 351-5476. E-mail: burns@env.med.nyu.edu

We thank M. Bosland for histologic diagnoses of the tumors and D. Gray and E. Cordisco for help with manuscript preparation.

This work was supported by National Institute of Environmental Health Sciences (NIEHS) grants ES09252 and ES10344 and is part of the Nelson Institute of Environmental Medicine and the Kaplan Cancer Center programs supported by grant CA16087 from the National Cancer Institute and center grant ES00260 from the NIEHS. A.N.U. was supported by a postdoctoral fellowship from the Cancer Research and Prevention Foundation, formerly known as the Cancer Research Foundation of America.

The authors declare they have no competing financial interests.

Received 12 August 2003; accepted 6 January 2004.

Materials and Methods

The protocol combined indefinite exposure to arsenic in drinking water with concomitant exposure to intermittent, topical UVR. The Hairless mice (strain Skh1) were fed sodium arsenite at various concentrations in drinking water starting at 21 days of age, as shown in Table 1. At 42 days of age (defined as time zero), the irradiations began on a Monday–Wednesday–Friday schedule at a dose of 1.0 kJ/m^2 UVR per exposure (solar spectrum). The UVR source was a bank of four fluorescent tubes (FS 20) mounted in parallel 15 cm apart. The mice were irradiated 30 cm below the source at a rate of 0.2 kJ/m^2/min. The dose was estimated to be about one-fourth the minimal erythemic dose for these mice. The mice were observed periodically for the presence of skin lesions, which were counted at each observation. The number of new tumors was obtained by subtracting the count at the previous observation. At the end of the experiment a large sample of tumors were examined histologically. More than 95% were diagnosed as squamous cell carcinomas.

Daily new cancer rates (R) in units of cancers per mouse per day were estimated for each interval by dividing the number of new tumors by the average number of mice alive and the length of the interval in days and were plotted at the midpoint of the intervals. Cumulative cancer yields (CY) were estimated by progressively summing the product of the rates and interval length in days. Standard deviations were estimated from the square root of the total cancers by assuming a Poisson distribution of cancers among mice. Linear regression analysis of the estimated new cancer rates was used to evaluate the parameters in Equation 1: the slope B, the length of the cancer-free interval t_0, and their respective standard deviations. Based on these values, cancer yields were calculated from Equation 2 and compared with the estimates of CY calculated as described above. Equation 2 is the time integral of Equation 1, and Equation 3 is 1 minus the first term in the Poisson distribution.

$$R = \text{new cancer rate} = B\,(t - t_0) \qquad [1]$$

$$\text{CY} = \text{cancer yield} = (1/2)\,B\,(t - t_0)^2 \qquad [2]$$

$$\text{PC} = \%\ \text{with cancer} = 100\,(1 - e^{-\text{CY}}) \qquad [3]$$

Results

Figure 1 shows mice selected randomly at 182 days from the UV-only group (Figure 1A) and the UV plus 1.25 mg/L group (Figure 1B). A lesion diameter of ≥ 2.0 mm was chosen as the criterion for distinguishing tumors from suspicious lesions. The arsenite affected both the number and size of the tumors, and even greater effects were noted at higher arsenite concentrations. Histologically, the tumors were squamous cell carcinomas as typically seen in mouse skin exposed to carcinogens (Rossman et al. 2001). Of the 322 cancers that were seen, 45 (~14%) showed especially rapid growth, whereas the remainder exhibited a distribution of growth rates. Some of the latter became almost indolent, reaching growth stasis at about 3–5 mm diameter but were nevertheless histologically distinguishable from papillomas and consistently showed local invasion.

Estimates of new cancer rates (cancers per mouse per day) in Figure 2 show typical variability of rate data but are fitted reasonably well with regression lines that extrapolate to an average time intercept of 93.6 ± 6.1 days (Table 1). The group receiving only UVR departed from the general upward trend of rate versus time in that after reaching a peak of 0.086 at 150.5 days, a decline to 0.029 was seen at the final two time points. A rate decrease after a peak cannot be accommodated by Equations 1 and 2, which necessitated not using the final time point. Justification for this discard is based on the observations that *a*) the UVR-only group developed the fewest cancers and would be subject to the greatest random fluctuations and *b*) a second experiment with a slightly higher UVR dose failed to show a similar rate decrease.

Overall, these data indicate that arsenite enhanced the yield of UVR-induced cancers in a multiplicative way with little effect on the temporal onsets; that is, the main effect of the arsenite was to increase the slope, B. A multiplicative effect is not unexpected for an enhancing agent that lacks carcinogenic activity of its own. Both the estimated and calculated yields are shown in Figure 3—estimated yields as data points and calculated yields as smooth curves based on Equation 2.

Although induced cancers in animals seem to be independent events, it is difficult to be sure that later cancers are not somehow influenced by the presence of earlier ones. One approach to assessing this problem is to use a Kaplan-Meier calculation that relies only on the first tumor on each animal, which by definition cannot be influenced by earlier tumors. The results of these calculations are shown in Figure 4. The relative lack of a dose dependence

Table 1. Summary of experimental and calculated cancer yields and tumor-free intervals.

UV (kJ/m^2)/ arsenite (mg/L)	Experimental yield ± SD at 182 days (cancers/animal)	Calculated yield ± SD at 182 days (cancers/animal)	Slope (cancers/ mouse/day^2)	Cancer-free interval (days)
1.0/0.00	2.40 ± 0.48	3.43 ± 1.94	0.00109279	103.4
1.0/1.25	5.40 ± 0.73	5.45 ± 0.79	0.00132573	91.3
1.0/2.50	7.21 ± 0.89	7.24 ± 1.35	0.00192710	95.3
1.0/5.00	11.10 ± 1.05	11.06 ± 1.25	0.00247784	87.5
1.0/10.0	6.80 ± 0.82	7.22 ± 2.38	0.00173550	90.8
				93.7[a]
1.7/0.00	3.47 ± 0.48	4.17 ± 1.09	0.00102334	91.8
1.7/10.0	9.56 ± 0.85	11.23 ± 2.62	0.00156513	62.2
				77.0[a]

[a]These numbers are averages of those preceding.

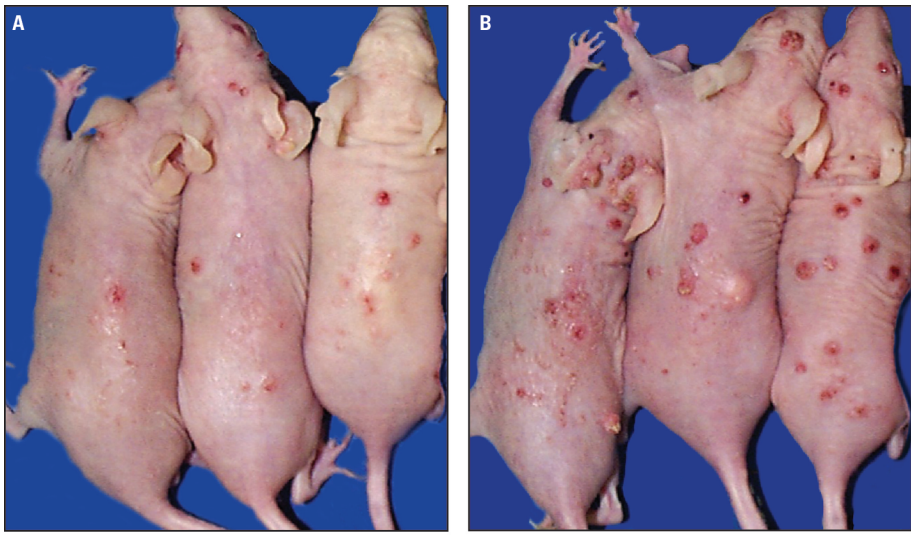

Figure 1. Typical cancer distributions in mice from (*A*) the UV-only group and (*B*) mice from the UV plus 1.25 mg/L arsenite group. Based on 2.0 mm diameter, there are five tumors in (*A*) and 14 tumors in (*B*). Even greater numbers of suspicious lesions are present, although quantitation is difficult on the photographs. Some suspicious lesions exhibit a growth burst into the tumor range within 2 weeks after cessation of UV exposures.

of t_0 (time intercepts) in Figure 2 reinforces the conclusion that the small temporal displacements are probably mostly associated with slope differences, not displacements along the time axis (t_0 values shown in Table 1). In the UVR-only group, 50% cancer incidence occurred at 140 days, whereas in the highest response group (UVR plus 5.0 mg/L), 50% incidence occurred at 109 days. In the 1.25, 2.50, and 10 mg/L groups (the latter not shown for clarity), the 50% incidence values were clustered near 120 days. The smooth lines in Figures 3 and 4 constitute families of curves. The closeness of the data points to the lines implies that reasonable estimates of slope B and time intercept t_0 can be derived from linear regression analysis of new cancer rates, despite the inherent variability of the rates themselves.

The dose–response relationship of squamous cell carcinoma yield as a function of arsenite concentration is shown in Figures 5 and 6, where the data are cancer yields expressed as cancers per mouse at 182 days versus arsenite concentration. The cancer yield was increased for all arsenite concentrations, and the peak enhancement as a ratio of yield for arsenite plus UVR versus UVR alone occurred at a concentration of 5.0 mg/L and represented a peak enhancement ratio of 4.63 ± 1.05. As the number and size of the cancers increase, mergers occur more frequently and undercounting becomes more likely. More than 10 cancers on a single animal generally could not be enumerated accurately.

Data from the ascending portion of Figure 5 are shown replotted in Figure 6 along with a regression analysis that shows 95% confidence interval (CI). The error bars were based on the square root of the total cancer counts by assuming a random distribution of cancers among the mice. The random assumption is predicated on uniform susceptibility from animal to animal and no interaction between multiple cancers on the same animal. The responses for estimated and calculated cancer yields are close, as can be seen in Table 1.

Data from a previously reported experiment and data from the present experiment are combined to show how cancer induction was altered as the UVR dose changed. Increasing the UVR dose by 1.70-fold increased the cancer yield by 1.45-fold, and the tumor-free interval decreased from 103.4 days to 91.8 days. A greater reduction in t_0 was seen for UVR with the arsenite, from 90.8 days to 62.2 days (Table 1). The arsenite enhancement at 10 mg/L was about the same for both UVR doses, averaging 2.79-fold.

At the end of the experiment, the UVR exposures were stopped and the arsenite was continued for an extra 2 weeks. Surprisingly, the growth rate of many of the cancers accelerated during this time, as if the UVR were retarding their growth. This makes sense because UVR is cytotoxic and would easily penetrate small cancers to a depth of a few millimeters.

Epidermal hyperplasia was measured on histologic preparations of skin samples obtained from the mice undergoing carcinogenesis testing and is shown in Figure 7. The sampling was performed by biopsy on day 183, 1 day after the final UVR exposure. Epidermal hyperplasia was seen in all groups that received either dietary arsenite or UVR.

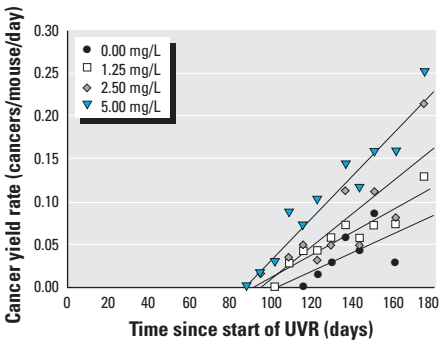

Figure 2. New cancer rates (R) after treatment with arsenite as a function of time showing linear regressions. The rate estimates are plotted at the midpoint of the observation intervals. Linear regression analysis was used to estimate the slope B, and the cancer-free interval t_0, and their respective SDs based on Equation 1. The highest arsenite concentration (10 mg/L) was omitted for clarity.

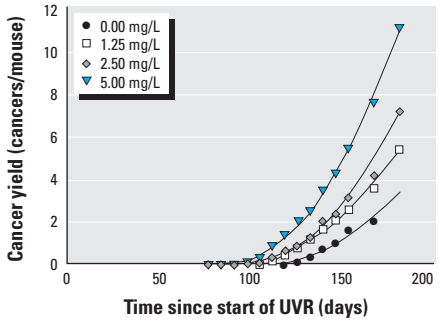

Figure 3. Cancer yield as a function of time for the various doses of arsenite (1.0 kJ/m^2 UVR). The points are estimated yield data, and the smooth curves were derived by plugging values for slope B and cancer-free interval t_0 into Equation 2.

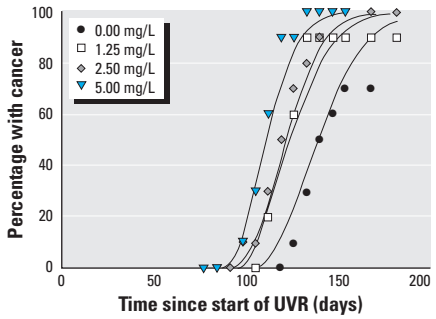

Figure 4. Kaplan-Meier analysis showing the percentage of mice with one or more cancers after treatment with arsenite. Estimates are shown as data points, whereas the smooth curves were derived by plugging values for B and t_0 into Equation 3. Each data point represents one mouse; there were 10 mice at each experimental group. UVR = 1.0 kJ/m^2 3 times weekly.

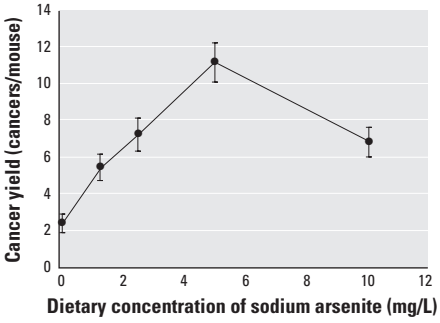

Figure 5. Dose–response data for estimated cancer yields at 182 days by the combination of 1.0 kJ/m^2 three times weekly and various concentrations of sodium arsenite continuously in drinking water showing the enhancement of the cancer yield by sodium arsenite. Error bars were derived from the square root of the total number of cancers.

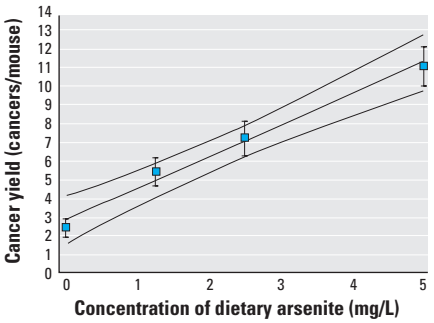

Figure 6. The ascending segment of the dose–response data in Figure 5 showing the enhancement of the cancer yield by sodium arsenite. A linear regression with 95% CIs is shown fitted to the data. The error bars were derived from the square roots of the total number of cancers. UVR = 1.0 kJ/m^2 3 times weekly.

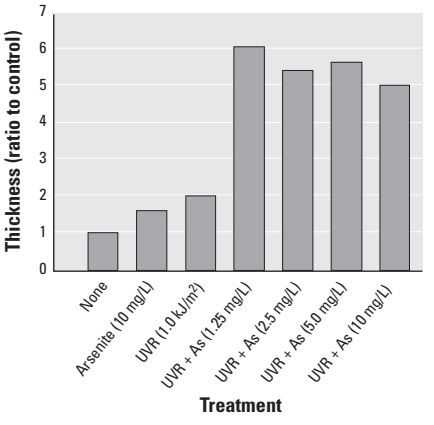

Figure 7. Epidermal hyperplasia in various treatment groups relative to no-treatment controls. The ordinate is the ratio of treated to control cell counts. Because the control epidermis is just a little more than one cell thick, the numbers are an approximate measure of the number of cell layers in the hyperplastic epidermis.

In mice receiving both agents, the hyperplasia was more than additive and often showed nonuniformity suggestive of early, microscopic neoplasms (Vega et al. 2001).

Discussion

Work with *in vitro* cell lines indicates that cyclin D1 is a key regulatory protein in controlling cell proliferation in several different cell types (Hunter and Pines 1994). Vogt and Rossman (2001) have reported that arsenite increases cyclin D1 expression in human fibroblasts. Arsenite may also activate signal transduction pathways upstream of cyclin D1 (Germolec et al. 1998; Simeonova and Luster 2000). Huang et al. (2001) reported that arsenite induces extracellular regulated kinase (ERK) activation through MAP kinase 6/p38–dependent pathways. Both arsenite and arsenate activated NFκB in mouse epidermal JB6 Cl41 cells but not in 30.7b cells, which are known to have low levels of ERKs, suggesting that ERK activation is involved in NFκB activation by arsenite (Huang et al. 2001).

Combined exposure of cells to arsenite and ionizing radiation showed that increased p53-dependent p21 expression, normally a block to cell cycle progression after DNA damage, was deficient and likely led to faulty DNA repair (Vogt and Rossman 2001). Many researchers have found that exposure of cells to nontoxic levels of arsenite enhances proliferation signaling (Barchowsky et al. 1999; Chen et al. 2001; Germolec et al. 1997, 1998; Vogt and Rossman 2001). The absence of normal p53 functioning coupled with growth stimulation likely contributes to defective DNA repair as well.

The dose–response relationship shown in Figure 5 is not unlike shapes seen for carcinogens in general—an initial increase up to a peak and then a decline at higher doses. Usually the decline is ascribed to the carcinogen's cytotoxic properties, which predominate over neoplastic effects at higher doses. However, no direct evidence of cytotoxicity was discernible in tissue sections taken 1 day after the final UVR exposure. For the concentration range from 0 to 5 mg/L arsenite in drinking water, the cancer enhancement was fitted quite well with a straight line.

It was surprising that arsenite caused equivalent levels of epidermal hyperplasia independent of concentration. Persistent hyperplasia is a hallmark of tumor promotion in mouse skin; however, others have shown with transgenically initiated mice that arsenite lacks even a hint of tumor-promoting activity, meaning that the hyperplasia was not likely part of a tumor promotion process (Germolec et al. 1998).

One hypothesis to explain the basis for the enhancing effect of arsenite on UVR carcinogenesis may involve a reversal of UVR-induced proliferative blockage (Hartwig et al. 2002). Cell cycle blockage is critical for preventing proliferation-dependent conversion of primary DNA damage to mutations and provides time for excision repair to remove much of the damage (Kaufmann 1995).

Skin epithelial cells exposed to long-term, intermittent UVR and dietary arsenite are probably experiencing a balance between simultaneous tendencies toward decreased and increased proliferation. UVR blocks proliferation as a result of DNA damage, whereas arsenite continuously stimulates proliferation, through the down-regulation of p21 and the up-regulation of the cyclin D1 pathway. The dose–response relationship for arsenite-induced cancer enhancement may depend on how effectively proliferative stimulation overcomes proliferative blockage.

The results reported here are the first demonstration of a linear relationship between arsenite concentration in drinking water and enhancement of the yield of squamous cell carcinomas in UVR-exposed mouse skin. The lowest concentration of arsenite used (1.25 mg/L) equals 721 μg/L arsenic, which is about 60 times the current allowable level (10 μg/L) in drinking water in the United States and is about 50% of the highest concentrations (~1,300 μg/L) found in Nevada drinking water (Warner et al. 1994) and about 20% of the highest concentrations (~3,400 μg/L) found in drinking water in the West Bengal region of India (Guha Mazumder et al. 1998). Arsenic-induced enhancement of carcinogenesis in the hairless mouse skin is one of the few instances where positive carcinogenicity in laboratory animals occurs at doses well within the range of human exposures. The results reported here are consistent with theoretical approaches that support a linear relationship between arsenite dose and cancer incidence in UV-exposed mouse skin. However, the quantitative application of the mouse data to humans ingesting high arsenite water is still fraught with difficulties related to species response differences. Although the arsenite-induced cancer enhancement in mouse skin was relatively independent of the UVR dose, the species dependence of this enhancement is unknown and could only be guessed for human skin.

References

Abernathy C, Liu Y, Longfellow D, Aposhian H, Beck B, Fowler B, et al. 1999. Arsenic: health effects, mechanisms of actions, and research issues. Environ Health Perspect 107:593–597.

Barchowsky A, Roussel R, Klei L, James P, Ganju N, Smith K, et al. 1999. Low levels of arsenic trioxide stimulate proliferative signals in primary vascular cells without activating stress effector pathways. Toxicol Appl Pharmacol 159(1):65–75.

Bau D, Wang T, Chung C, Wang A, Jan K. 2002. Oxidative DNA adducts and DNA–protein cross-links are the major DNA lesions induced by arsenite. Environ Health Perspect 110(suppl 5):753–756.

Brown K, Boyle K, Chen C, Gibb H. 1989. A dose-response analysis of skin cancer from inorganic arsenic in drinking water. Risk Anal 9(4):519–528.

Brown K, Guo H, Kuo T, Greene H. 1997. Skin cancer and inorganic arsenic: uncertainty-status of risk. Risk Anal 17(1):37–42.

Buchet J, Lison D. 2000. Clues and uncertainties in the risk assessment of arsenic in drinking water [Review]. Food Chem Toxicol 38:81–85.

Chen H, Liu J, Merrick B, Waalkes M. 2001. Genetic events associated with arsenic-induced malignant transformation: applications of cDNA microarray technology. Mol Carcinog 30(2):79–87.

Chiou H, Chiou S, Hsu Y, Chou Y, Tseng C, Wei M, et al. 2001. Incidence of transitional cell carcinoma and arsenic in drinking water: a follow-up study of 8,102 residents in an arseniasis-endemic area in northeastern Taiwan. Am J Epidemiol 153(5):411–418.

Corsini E, Asti L, Viviani B, Marinovich M, Galli C. 1999. Sodium arsenate induces overproduction of interleukin-1alpha in murine keratinocytes: role of mitochondria. J Invest Dermatol 113(5):760–765.

Germolec D, Spalding J, Boorman G, Wilmer J, Yoshida T, Simeonova P, et al. 1997. Arsenic can mediate skin neoplasia by chronic stimulation of keratinocyte-derived growth factors. Mutat Res 386(3):209–218.

Germolec D, Spalding J, Yu H, Chen G, Simeonova P, Humble M, et al. 1998. Arsenic enhancement of skin neoplasia by chronic stimulation of growth factors. Am J Pathol 153(6):1775–1785.

Guha Mazumder D, Haque R, Ghosh N, De B, Santra A, Chakraborty D, et al. 1998. Arsenic levels in drinking water and the prevalence of skin lesions in West Bengal, India. Int J Epidemiol 27(5):871–877.

Hartwig A, Asmuss M, Ehleben I, Herzer U, Kostelac D, Pelzer A, et al. 2002. Interference by toxic metal ions with DNA repair processes and cell cycle control: molecular mechanisms. Environ Health Perspect 110:797–799.

Hei T, Liu S, Waldren C. 1998. Mutagenicity of arsenic in mammalian cells: role of reactive oxygen species. Proc Natl Acad Sci USA 95(14):8103–8107.

Hu Y, Su L, Snow E. 1998. Arsenic toxicity is enzyme specific and its affects on ligation are not caused by the direct inhibition of DNA repair enzymes. Mutat Res 408:203–218.

Huang C, Li J, Ding M, Wang L, Shi X, Castranova V, et al. 2001. Arsenic-induced NFκB transactivation through Erks- and JNKs-dependent pathways in mouse epidermal JB6 cells. Mol Cell Biochem 222(1–2):29–34.

Huff J, Chan P, Waalkes M. 1998. Arsenic carcinogenicity testing [Letter]. Environ Health Perspect 106:A170.

Hunter T, Pines J. 1994. Cyclins and cancer II: cyclin D and CDK inhibitors come of age. Cell 79:573–582.

Kaufmann W. 1995. Cell cycle checkpoints and DNA repair preserve the stability of the human genome [Review]. Cancer Metastasis Rev 14(1):31–41.

Li J, Rossman T. 1989a. Inhibition of DNA ligase activity by arsenite: a possible mechanism of its comutagenesis. Mol Toxicol 2(1):1–9.

———. 1989b. Mechanism of comutagenesis of sodium arsenite with *N*-methyl-*N*-nitrosourea. Biol Trace Element Res 21:373–381.

———. 1991. Comutagenesis of sodium arsenite with ultraviolet radiation in Chinese hamster V79 cells. Biol Metals 4:197–200.

Maier A, Schumann B, Chang X, Talaska G, Puga A. 2002. Arsenic co-exposure potentiates benzo[*a*]pyrene genotoxicity. Mutat Res 517(1–2):101–111.

Mure K, Uddin A, Lopez L, Styblo M, Rossman T. 2003. Arsenite induces delayed mutagenesis and transformation in human osteosarcoma cells at extremely low concentrations. Environ Mol Mutagen 41(5):322–331.

National Research Council. 1999. Risk Assessment of Arsenic in Drinking Water: Subcommittee on Arsenic in Drinking Water. Washington, DC:National Academy Press.

Rossman T. 1981. Enhancement of UV-mutagenesis by low concentrations of arsenite in *E. coli*. Mutat Res 91:207–211.

———. 1989. On the mechanism of the comutagenic effect of Cu(II) with ultraviolet light. Biol Trace Elem Res 21:383–388.

———. 2003. Mechanism of arsenic carcinogenesis: an integrated approach. Mutat Res 533:37–66.

Rossman T, Uddin A, Burns F, Bosland M. 2001. Arsenite is a cocarcinogen with solar ultraviolet radiation for mouse skin: an animal model for arsenic carcinogenesis. Toxicol Appl Pharmacol 176(1):64–71.

———. 2002. Arsenite cocarcinogenesis: an animal model

derived from genetic toxicology studies. Environ Health Perspect 110(suppl):749–752.

Schlatterer K, Schlatterer B, Krauter G, Hecker E, Chandra P. 2000. A novel polypeptide p10 expressed in tumor-promoter-treated murine epidermis and in untreated neonatal murine epidermis. Anticancer Res 20(1A):289–292.

Simeonova P, Luster M. 2000. Mechanisms of arsenic carcinogenicity: genetic or epigenetic mechanisms. J Environ Pathol Toxicol Oncol 19(3):281–286.

Tucker S, Lamm S, Li F, Wilson R, Byrd D, Lai S, et al. 2001. Relationship between Consumption of Arsenic-Contaminated Well Water and Skin Disorders in Huhhot, Inner Mongolia. Cambridge, MA:Inner Mongolia Cooperative Arsenic Project. Available: http://phys4harvard.edu/~wilson/arsenic/references/IMCAP_report.html :1–27 [accessed 1 December 2003].

Vega L, Styblo M, Patterson R, Cullen W, Wang C, Germolec D. 2001. Differential effects of trivalent and pentavalent arsenicals on cell proliferation and cytokine secretion in normal human epidermal keratinocytes. Toxicol Appl Pharmacol 172(3):225–232.

Viren J, Silvers A. 1999. Nonlinearity in the lung cancer dose-response for airborne arsenic: apparent confounding by year of hire in evaluating lung cancer risks from arsenic exposure in Tacoma smelter workers. Regul Toxicol Pharmacol 30(2 pt 1):117–129.

Vogt B, Rossman T. 2001. Effects of arsenite on p53, p21 and cyclin D expression in normal human fibroblasts—a possible mechanism for arsenite's comutagenicity. Mutat Res 478(1–2):159–168.

Warner M, Moore L, Smith M, Kalman D, Fanning E, Smith A. 1994. Increased micronuclei in exfoliated bladder cells of individuals who chronically ingest arsenic-contaminated water in Nevada. Cancer Epidemiol Biomarkers Prev 3(7):583–590.

Yager J, Wiencke J. 1993. Enhancement of chromosomal damage by arsenic: implications for mechanism. Environ Health Perspect 101(suppl 3):79–82.

———. 1997. Inhibition of poly(ADP-ribose) polymerase by arsenite. Mutat Res 386(3):345–351.